

Normally-off AlGaIn/GaN MIS-HFETs Using Non-polar *a*-Plane

Masayuki Kuroda, Tetsuzo Ueda, and Tsuyoshi Tanaka

Semiconductor Device Research Center, Semiconductor Company, Matsushita Electric Industrial Co., Ltd.
1 Kotari-yakimachi, Nagaokakyo-shi, Kyoto 617-8520, Japan
Phone: +81-75-956-9055 Fax: +81-75-956-9110 E-mail: kuroda.masayuki@jp.panasonic.com

1. Introduction

AlGaIn/GaN hetero-junction field effect transistors (HFETs) are promising for power switching applications owing to the high breakdown voltage and high saturation electron velocity of the material system. Conventional GaN-based HFETs were formed on polar (0001) *c*-planes on which the spontaneous and piezoelectric polarization fields produce the extraordinary high sheet carrier concentration. So far normally-on HFETs with low on-state resistance and high breakdown voltage have been reported taking advantages of the inherent high sheet charge density [1].

Considering practical power switching applications, normally-off operations are strongly required for the safety operation. As one of the technical solutions for the normally-off HFETs, we have demonstrated the AlGaIn/GaN HFETs on non-polar (11-20) *a*-plane which is free from the above mentioned large polarization [2]. The use of the non-polar plane serves better controllability of the carrier concentration so that the normally-off operation would be easily achieved. However, the reported non-polar HFET does not exhibit complete normally-off as well as the drain current is significantly low due to the poor channel mobility.

In this paper, we report on normally-off operation of non-polar *a*-plane AlGaIn/GaN MIS-HFETs with threshold voltage of +1.3 V. High drain current of 112 mA/mm is also achieved in a recessed gate metal-insulator-semiconductor (MIS) HFET with the improved crystal quality on thick AlN buffer layers.

2. MOCVD growths of *a*-plane AlGaIn/GaN HFETs

In order to improve crystalline quality of *a*-plane GaN, we introduce high-temperature grown thick AlN buffer layers instead of the previously reported low-temperature grown GaN buffer layers. Prior to the device fabrication, we examine the effect of the AlN buffer thickness on the crystal quality of the overgrown GaN.

Figure 1 shows a typical X-ray diffraction pattern of the AlGaIn/GaN grown on the (1-102) *r*-plane sapphire with the AlN buffer layer, in which no crystallographic plane other than *a*-plane is observed. FWHM of rocking curve and surface roughness measured by atomic force microscope (AFM) are measured for the *a*-plane GaN grown with various AlN thickness as shown in figure 2. The crystal quality and the surface roughness are significantly improved by the thick AlN buffer up to 1 μm . It is noted that the lowest FWHM of 608 arcsec is obtained for the 8- μm -thick *a*-plane GaN, which is one of the lowest value for the *a*-plane GaN without selective lateral growths [3]. Figure 3 compares the surface morphology of *a*-plane GaN on high-temperature AlN and low-temperature GaN, implying that surface flatness is improved by the AlN buffer. In addition, Hall mobility is increased to 87 cm^2/Vs

in n-AlGaIn/GaN on the AlN buffer layer from 46 cm^2/Vs on the low-temperature GaN buffer.

3. Fabrication of normally-off *a*-plane MIS-HFETs

Figure 4 shows the schematic cross section of the fabricated *a*-plane MIS-HFET on *r*-plane sapphire. A recessed gate structure with highly conductive n-GaN capping layers is employed for the *a*-plane HFET to increase the drain current and to reduce series resistance. The MIS structure with Si_xN_y as an insulator enables to apply high positive gate voltage resulting in higher maximum drain current as compared with conventional Schottky-gate HFETs. Note that thin AlN space layer is placed between the AlGaIn and GaN to suppress the alloy scattering. Figure 5 shows the $I_{\text{ds}}-V_{\text{ds}}$ characteristics of the fabricated *a*-plane MIS-HFET, in which complete normally-off operation with the threshold voltage of +1.3 V is confirmed. High maximum drain current of 112 mA/mm is achieved by the recessed-gate structure as well. Figure 6 is the comparison of the $I_{\text{ds}}-V_{\text{gs}}$ characteristics between the recessed gate non-polar MIS-HFET and the previously reported Schottky-gate non-polar HFET. This figure implies that the use of the recessed-gate MIS structure on thick AlN buffer instead of the conventional low-temperature GaN buffer drastically improves the device performance.

4. Conclusions

We successfully demonstrated AlGaIn/GaN MIS-HFETs on non-polar *a*-plane. The device employs the recessed gate structure with highly conducting capping layers as well as it is grown on thick AlN buffer which improves the crystal quality. The fabricated device exhibits complete normally-off operation with the threshold voltage of +1.3 V and the high maximum drain current of 112 mA/mm. The demonstrated non-polar MIS-HFETs are promising for the future power switching application.

Acknowledgements

The authors would like to express sincere thanks to Dr. Daisuke Ueda for his technical advice and continuing support throughout this work.

References

- [1] M. Hikita, M. Yanagihara, K. Nakazawa, H. Ueno, Y. Hirose, T. Ueda, Y. Uemoto, T. Tanaka, D. Ueda, and T. Egawa, IEEE Trans. Electron Devices, **52** (2005) 1963.
- [2] M. Kuroda, H. Ishida, T. Ueda, T. Tanaka, Ext. Abst. of SSDM., (2005) 470.
- [3] B. M. Imer, F. Wu, S. P. DenBaars, J. S. Speck, Appl. Phys. Lett. **88** (2006) 061908.

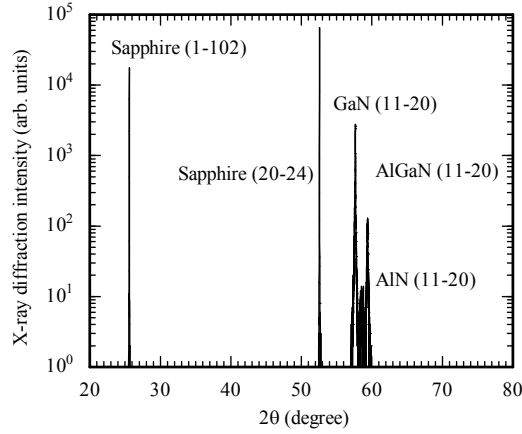


Figure 1. X-ray diffraction pattern of an *a*-plane $\text{Al}_{0.26}\text{Ga}_{0.74}\text{N}$ 25nm/GaN 3 μm /AlN 500 nm epilayers grown on an *r*-plane sapphire.

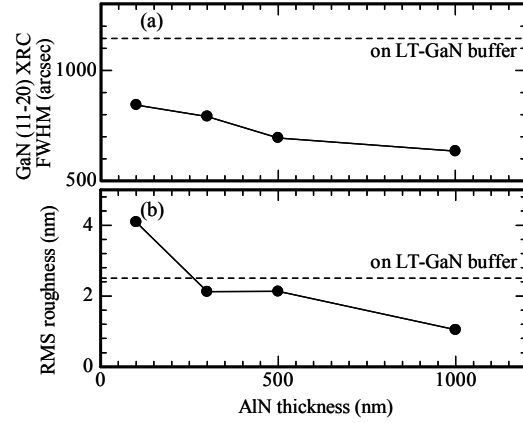


Figure 2. (a) Full width of half maximum of the X-ray diffraction rocking curve (3- μm -thick (11-20) GaN) and (b) surface roughness measured by AFM as a function of AlN buffer layer thickness.

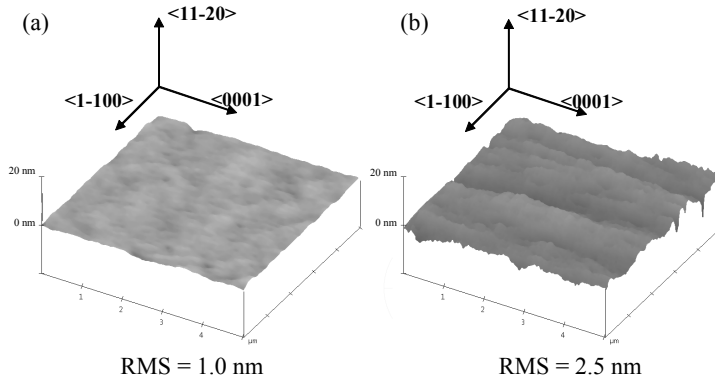


Figure 3. AFM images of the surface of non-polar *a*-plane GaN on (a) high-temperature AlN buffer, (b) low-temperature GaN.

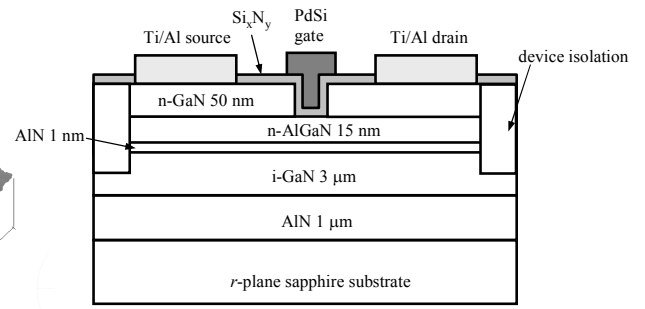


Figure 4. Schematic cross section of the fabricated *a*-plane AlGaIn/GaN MIS-HFET.

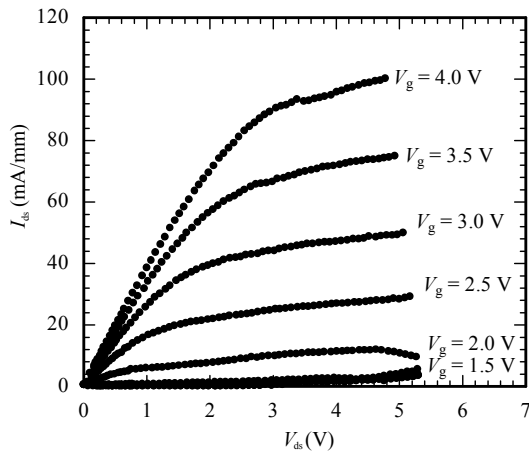


Figure 5. I_{ds} - V_{ds} characteristics of the fabricated *a*-plane AlGaIn/GaN MIS-HFET.

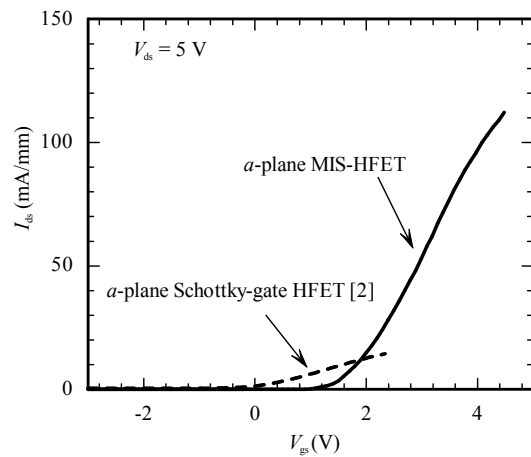


Figure 6. I_{ds} - V_{gs} characteristics of the *a*-plane AlGaIn/GaN MIS-HFET as compared with that of the reported Schottky-gate *a*-plane HFET.